Hindawi
Geofluids
Volume 2022, Article ID 4703957, 11 pages
https://doi.org/10.1155/2022/4703957

Research Article

Study on the Synchronous Instability Mechanism of the Coal Wall and Direct Roof of High Soft Coal Seam

Baojie Fu ,[1,2] Jiawen Li,[1,2] Min Tu ,[1,2] and Ningping Jin[1,2]

[1]*School of Mining Engineering, Anhui University of Science and Technology, Road Taifeng No. 168, Huainan, Anhui 232001, China*
[2]*Key Laboratory of Coal Mine Safety and Efficiently Caving of Ministry of Education, Anhui University of Science and Technology, Huainan, Anhui 232001, China*

Correspondence should be addressed to Baojie Fu; bjfu@aust.edu.cn

Received 4 January 2022; Accepted 13 February 2022; Published 2 March 2022

Academic Editor: Zhijie Wen

The advanced mining stress on a large working face can easily lead to the failure of the roof and coal mass; coal wall spalling and roof caving occur. The degree of coal wall failure and the depth of the plastic fracture zone are closely related to the advanced mining stress. The mechanical analysis model is established, and the stress distribution in the fracture and plastic zone is analyzed by the elastic-plastic theory, and the depth function expressions of two zones are determined. Comparative analysis of the factors affecting mining strength shows that the mining depth, mining height, and strength of coal are the key factors affecting the stability of the coal wall. The A1 coal of Zhangji mine in Huainan is soft and thick, and the direct roof is easily separated by the organic membrane, which is easy to form arc-shaped sliding instability. The increase in the unsupported roof area causes the direct roof caving and reduces its bearing capacity and stiffness. It is unable to provide enough support for the broken block of the overlying key stratum, which makes the broken block reverse rotation and further aggravate the roof fall; the synchronous instability of the coal wall and direct roof is formed.

1. Introduction

A large mining height working face has large stope space, the scope of roof collapse and the movement range of fractured rock strata will be greatly increased, the filling degree of goaf is reduced, and it has an impact on the fracture law and structural characteristics of overburden. In particular, when the roof has multilayer thick and hard rock and one or both sides of the working face are empty, it will lead to abnormal pressure such as spalling and roof caving, which has been proven in the previous mining practice of 4~6 m mining height[1–4]. With the increase in mining height, the depth and frequency of coal wall spalling will undoubtedly be increased, and the leakage of the broken roof will be intensified, which will seriously limit the advancing speed of the working face and form a vicious circle.

The influence of overlying rock structure on the stability of surrounding rock in large mining height has hanged fundamentally, and the surrounding rock control mechanism will also change. Professor Wang Jiachen [5, 6] carried out mechanical analysis and experimental research on the occurrence conditions of "two hard" coal seams, established the elastic thin plate mechanical model of the first roof caving, studied the characteristics of sectional weighting of roof strata in different areas along the length direction of the working face, and analyzed the reasons of roof stratum migration and weighting. Yan et al. [7] established the "short cantilever beam+hinged rock beam" model of a rock layer fracture in a large mining height working face by means of numerical simulation and theoretical analysis. Through field observation, theoretical analysis, and numerical simulation analysis of the large mining height working face, Yan et al. [8, 9] studied the law of mine pressure behavior, the influence range of advanced abutment pressure, and the position of the peak point in the fully mechanized mining face and considered that the basic roof weighting of the fully mechanized mining face with large mining height is more severe than that of the ordinary fully mechanized mining face, and the coal wall spalling and roof caving are more serious, and the hydraulic pressure is more serious; there is a common phenomenon of dynamic load impact on the support. Based on the D-P-Y criterion and limit equilibrium theory of plasticity mechanics, Bo et al. [10, 11] analyzed the width of the plastic failure zone and stress distribution of the coal wall, obtained the calculation method of the width of the plastic failure zone of the coal wall and abutment pressure in front of the working face, and analyzed the failure process and control measures of the roof and wall of "three soft coal seams". Fang et al. [12] established the mechanical model of surrounding rock hydraulic support structure, analyzed the whole process of coal wall deformation-rupture-failure-instability, analyzed the arc sliding instability process of the upper part of the coal wall by the stability coefficient method, and calculated the critical height of coal wall stability. There are mainly four methods [13, 18] to control the stability of the coal wall and roof of the large mining height working face. Change the stress environment of the working face, and appropriately improve the support resistance. Through the coal wall and roof grouting, use an anchor rod (such as bamboo anchor rod) and other means to improve the coal and rock rest cohesive force. A step coal wall mining method reduces the time of coal wall stability maintenance and reduces the mining height. Improve mining technology to speed up the advance, reduce the length of the working face, use the bow mining, improve the speed of the shearer, and reduce the cutting depth and other measures. Based on the elastic-plastic theory, this paper analyzes the stress distribution law of coal and rock mass and the depth of the plastic failure zone under the action of advanced mining stress and defines the main control factors affecting the failure of the coal wall with large mining height. Combined with the occurrence conditions of specific coal seam, the synchronous instability mechanism of the coal wall and roof in the large mining height working face of soft coal is expounded, and the main control measures are proposed.

2. Advanced Mining Stress Distribution Law of the Large Mining Height Working Face

With the mining of the working face, the goaf will be formed; the stress load of the overlying strata gradually transfers to the coal and rock mass around the working face. According to the stress redistribution characteristics, the stress completely acts on the coal and rock mass in front of and on the side of the working face, thus forming a large range of stress concentration in these areas. In general, the stress concentration factor is $k = 2 \sim 4$. Under the influence of the advance pressure, mining stress increasing and reducing area is formed in the coal body and its roof and floor, and they move forward continuously with the mining. According to the total stress-strain curve of coal and rock, its deformation can be divided into three stages: elastic stage, plastic stage, and failure residual stage. When the abutment pressure does not exceed the ultimate bearing capacity of coal, the coal body is in AN elastic state; when the coal mass reaches the yield condition but fails to meet the fracture requirements, the coal mass is in the plastic stage; when the deformation of the coal body reaches the fracture condition, the coal mass is in the fracture state. The fracture zone, plastic zone, elastic zone, and original rock stress zone can be produced in coal mass, as shown in Figure 1.

3. Mechanics Analysis of the Coal Wall of the Large Mining Height Working Face

3.1. Mechanics Analysis of the Coal Wall of Stability. The failure degree of the coal wall and the width of the plastic fracture zone are closely related to the magnitude of mining advance stress. As shown in Figure 2, the mechanical analysis model of the coal wall is established, x_b is the boundary between the broken zone and the plastic zone, and x_p is the boundary between the plastic zone and the elastic zone.

As shown in Figure 2(b), considering the vertical stress σ_y, horizontal resistance P_i, horizontal stress σ_x, and shear stress τ caused by upper and lower boundary dislocation, the microelement equilibrium equation is established:

$$-m(\sigma_x + d\sigma_x) + m\sigma_x + 2\tau dx = 0, \tag{1}$$

where m is the coal thickness.

Shear stress τ caused by upper and lower boundary dislocation is

$$\tau = f d\sigma_y, \tag{2}$$

where f is the friction resistance coefficient of upper and lower boundary dislocation.

Equation (3) can be obtained through [8] and [10]:

$$d\sigma_x = \frac{2f}{m}\sigma_y dx, \tag{3}$$

namely, $\beta = 2f/m$. The above formula is as follows:

$$d\sigma_x = \beta\sigma_y dx. \tag{4}$$

In the broken area ($0 \le x \le x_b$), the medium of coal and rock mass meets the following requirements:

$$\sigma_y^b = K_p\sigma_x^b + \sigma_c^*, \tag{5}$$

where C^* is the medium cohesion in the broken zone and φ is the internal friction angle, namely, $K_p = (1 + \sin\varphi)/(1 - \sin\varphi)$ and $\sigma_c^* = 2C^* \cos\varphi/(1 - \sin\varphi)$.

Equation (5) is substituted into equation (3) to obtain

$$d\sigma_x^b = \beta K_p\sigma_x^b + \beta\sigma_c^*. \tag{6}$$

The general explanation is

$$\sigma_x^b = -\frac{\sigma_c^*}{K_p} + C_1 e^{\beta K_p x}. \tag{7}$$

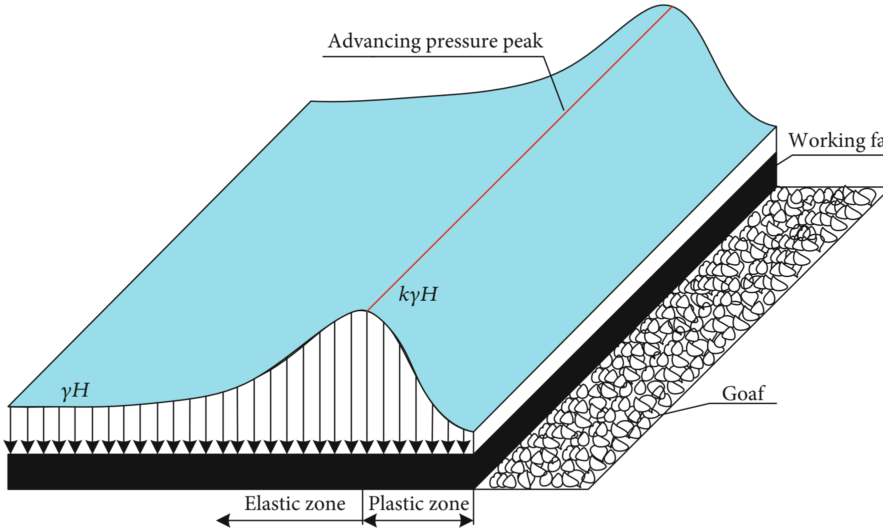

FIGURE 1: Stress distribution of stope.

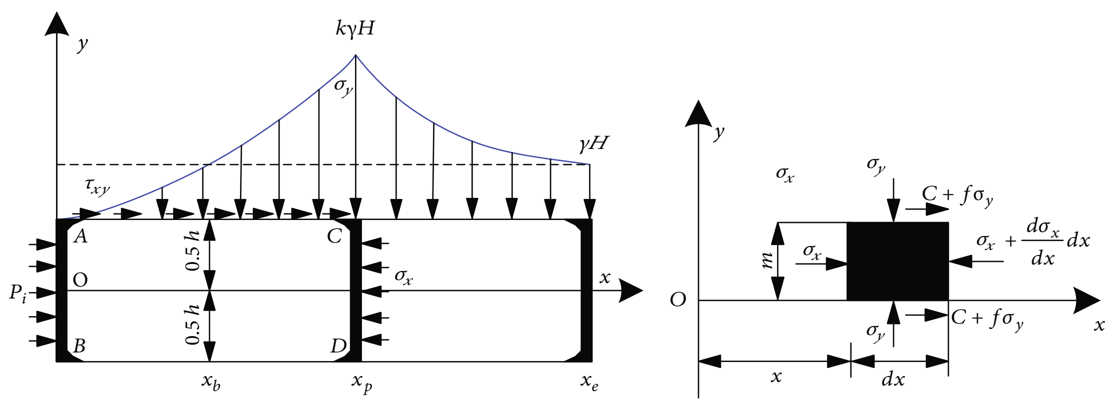

(a) The stress distribution

(b) Mechanical model

FIGURE 2: Stress analysis model of coal mass.

When $x = 0$, $\sigma_x^b|_{x=0} = P_i$, and substitute it into equation (7) to obtain

$$C_1 = P_i + \frac{\sigma_c^*}{K_p}. \tag{8}$$

The stress of coal mass at the edge of the fracture area is

$$\begin{cases} \sigma_x^b = -\dfrac{\sigma_c^*}{K_p} + \left(P_i + \dfrac{\sigma_c^*}{K_p}\right) e^{\beta K_p x}, \\ \sigma_y^b = \dfrac{d\sigma_x}{\beta dx} = K_p \left(P_i + \dfrac{\sigma_c^*}{K_p}\right) e^{\beta K_p x}, \end{cases} \quad (0 \le x \le x_b). \tag{9}$$

In the plastic zone ($x_b \le x \le x_p$), the medium of coal mass meets the following requirements:

$$\sigma_y^p = K_p \sigma_x^p + \sigma_c - M_0 \varepsilon_p, \tag{10}$$

where M_0 is the softening modulus of coal and S_z is the strain gradient of coal in the plastic zone, namely, $S_z = \tan(\alpha)$ and $\varepsilon_p = (S_z/m)(x_p - x)$. α is the sum of deformation angles of the coal roof and floor in the plastic zone.

The above formula is

$$\sigma_y^p = K_p \sigma_x^p + \sigma_c - \frac{M_0 S_z}{m}(x_p - x). \tag{11}$$

Equation (11) is substituted into equation (4) to obtain

$$d\sigma_x^p = \beta K_p \sigma_x^p + \beta\left[\sigma_c - \frac{M_0 S_z}{m}(x_p - x)\right]. \tag{12}$$

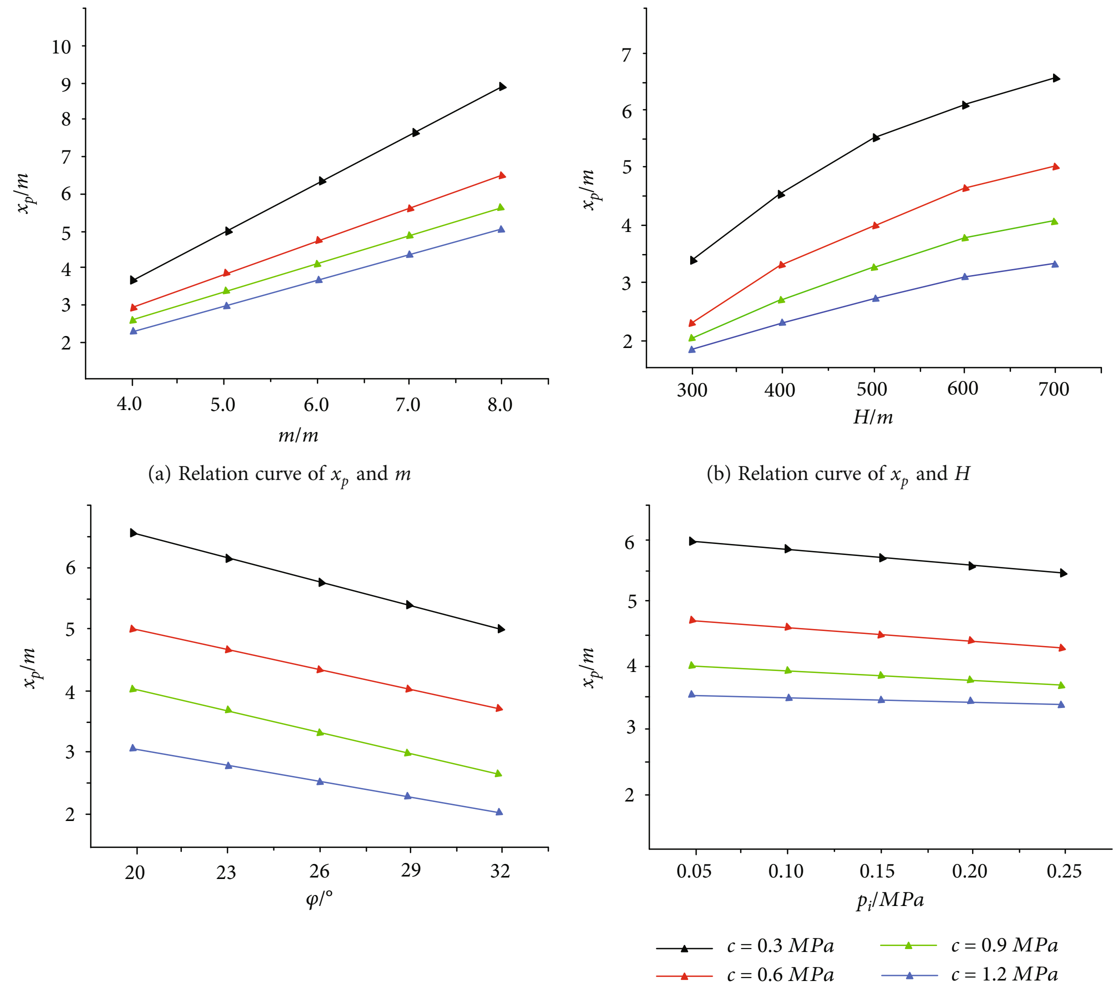

(a) Relation curve of x_p and m

(b) Relation curve of x_p and H

(c) Relation curve of x_p and φ

(d) Relation curve of x_p and p_i

FIGURE 3: Analysis of influencing factors of x_p.

Therefore, the stress state of coal in the plastic zone can be expressed as

$$\begin{cases} \sigma_x^p = \left(\dfrac{(M_0S_z/m)(x_p - x)}{K_p}\right) - \\ \dfrac{\beta(M_0S_z/m) + \beta^2 K_p \sigma_c}{(\beta K_p)^2} + C_2 e^{\beta K_p x} \quad (x_b \le x \le x_p), \\ \sigma_y^p = -\dfrac{M_0 S_z}{m\beta K_p} + C_2 K_p e^{\beta K_p x}. \end{cases} \tag{13}$$

At the boundary of the plastic and elastic zone ($x = x_p$), the destruction of coal is subject to

$$\sigma_y^p\Big|_{x=x_p} = K_p \sigma_x^p + \sigma_c, \tag{14}$$

where σ_c is the residual strength of coal, namely, $\sigma_c = 2C \cos\varphi/(1 - \sin\varphi)$, and C is the cohesion.

When $x = x_p$, $\sigma_y^p|_{x=x_p} = K\gamma H$, where K is the stress concentration factor and γH is the original rock stress.

Equation (14) is written as

$$C_2 = \frac{(M_0S_z/m\beta K_p) + K\gamma H}{K_p} e^{-\beta K_p x_p}. \tag{15}$$

The stress state of coal in the plastic region can be expressed as

$$\begin{cases} \sigma_x^p = \left(\dfrac{(M_0S_z/m)(x_p - x)}{K_p}\right) - \left(\dfrac{\beta(M_0S_z/m) + \beta^2 K_p \sigma_c}{(\beta K_p)^2}\right) + \\ \left(\dfrac{\beta(M_0S_z/m) + \beta^2 K_p K\gamma H}{(\beta K_p)^2}\right) e^{\beta K_p (x - x_p)} \quad (x_b \le x \le x_p), \\ \sigma_y^p = -\dfrac{M_0 S_z}{m\beta K_p} + \left(\dfrac{(M_0S_z/m) + K_p \beta K\gamma H}{\beta K_p}\right) e^{\beta K_p (x - x_p)}. \end{cases} \tag{16}$$

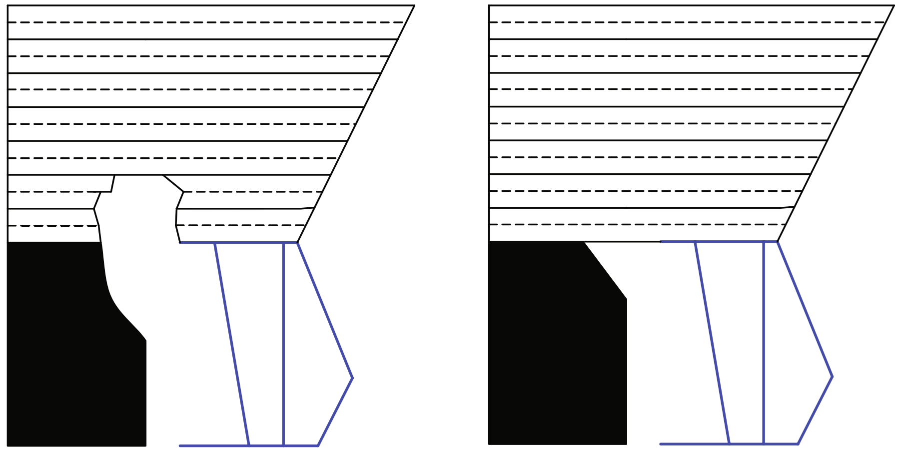

(a) Synchronous instability of the coal wall and roof (b) Instability of the coal wall under high shear stress

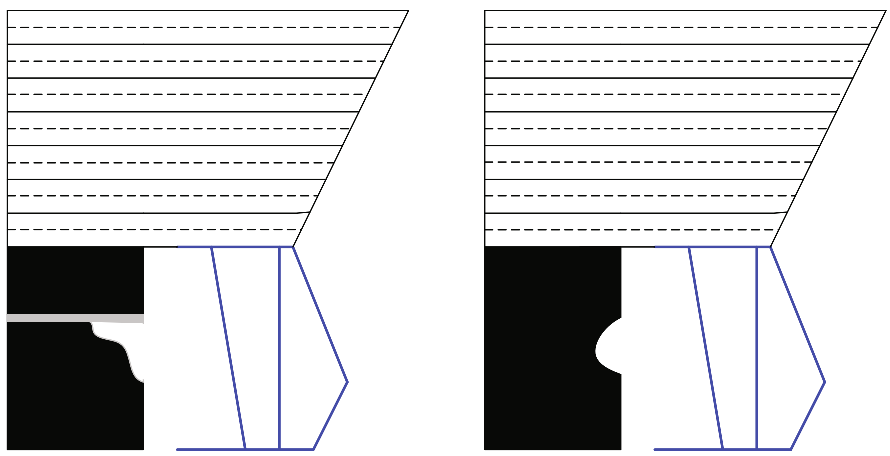

(c) Instability of the coal wall affected by gangue (d) Instability of the coal wall caused by tensile cracking

Figure 4: Coal wall spalling type.

When $x = x_b$,

$$\sigma_y^b\Big|_{x=x_b} = K_p \sigma_x^b\Big|_{x=x_b} + \sigma_c - \frac{M_0 S_z}{m}\left(x_p - x_b\right), \tag{17}$$

so

$$K_p\left(P_i + \frac{\sigma_c^*}{K_p}\right)e^{\beta K_p x_b} = K_p\left[-\frac{\sigma_c^*}{K_p} + \left(P_i + \frac{\sigma_c^*}{K_p}\right)e^{\beta K_p x_b}\right] + \sigma_c - \frac{M_0 S_z}{m}\left(x_p - x_b\right). \tag{18}$$

The solution of equation (18) is

$$x_p - x_b = \frac{m\left(\sigma_c - \sigma_c^*\right)}{M_0 S_z}. \tag{19}$$

When $x = x_b$, $\sigma_x^b\big|_{x=x_b} = \sigma_x^p\big|_{x=x_b}$.

$$\begin{aligned} -\frac{\sigma_c^*}{K_p} + \left(P_i + \frac{\sigma_c^*}{K_p}\right)e^{\beta K_p x_b} = {} & \left(\frac{\left(M_0 S_z/m\right)\left(x_p - x_b\right)}{K_p}\right) \\ & - \left(\frac{\beta\left(M_0 S_z/m\right) + \beta^2 K_p \sigma_c}{\left(\beta K_p\right)^2}\right) \\ & + \left(\frac{\beta\left(M_0 S_z/m\right) + \beta^2 K_p K \gamma H}{\left(\beta K_p\right)^2}\right) e^{\beta K_p \left(x_b - x_p\right)}. \end{aligned} \tag{20}$$

Equation (20) is substituted into equation (19) to obtain

$$\begin{aligned} -\frac{\sigma_c^*}{K_p} + \left(P_i + \frac{\sigma_c^*}{K_p}\right)e^{\beta K_p x_b} = {} & \frac{\left(\sigma_c - \sigma_c^*\right)}{K_p} \\ & - \left(\frac{\beta\left(M_0 S_z/m\right) + \beta^2 K_p \sigma_c}{\left(\beta K_p\right)^2}\right) \\ & + \left(\frac{\beta\left(M_0 S_z/m\right) + \beta^2 K_p K \gamma H}{\left(\beta K_p\right)^2}\right) e^{-\frac{m \beta K_p \left(\sigma_c - \sigma_c^*\right)}{M_0 S_z}}. \end{aligned} \tag{21}$$

The depth of the coal broken and plastic zone is expressed as

$$\begin{cases} x_b = \dfrac{1}{\beta K_p} \ln \left[-\left(\dfrac{\beta M_0 S_z}{m(\beta K_p)^2 (P_i + (\sigma_c^*/K_p))} \right) + \left(\dfrac{\beta (M_0 S_z/m) + \beta^2 K_p K \gamma H}{(\beta K_p)^2 (P_i + (\sigma_c^*/K_p))} \right) e^{-\frac{m\beta K_p (\sigma_c - \sigma_c^*)}{M_0 S_z}} \right], \\ x_p = \dfrac{m(\sigma_c - \sigma_c^*)}{M_0 S_z} + \dfrac{1}{\beta K_p} \ln \left[-\left(\dfrac{\beta M_0 S_z}{m(\beta K_p)^2 (P_i + (\sigma_c^*/K_p))} \right) + \left(\dfrac{\beta (M_0 S_z/m) + \beta^2 K_p K \gamma H}{(\beta K_p)^2 (P_i + (\sigma_c^*/K_p))} \right) e^{-\frac{m\beta K_p (\sigma_c - \sigma_c^*)}{M_0 S_z}} \right]. \end{cases} \quad (22)$$

3.2. Case Analysis. The coal mass of group A of Zhangji mine has low strength, the thick roof layer is directly covered with fine sandstone, horizontal bedding is developed, the layer is sandwiched with argillaceous bands, argillaceous inclusions, and organic membrane, and the relevant parameters are taken as follows: $f_b = 0.5$, $n_b = 0.6$ MPa, $f_p = 0.25$, $n_p = 0.24$ MPa, $C^* = 0.2$ MPa, $\varphi = 22.4°$, $M_0 = 0.1$ GPa, $\alpha = 12°$, and $K = 2.3$.

(1) When $H = 500$ m, $P_i = 0.1$ MPa, and $\varphi = 24°$, as shown in Figure 3(a), with the same cohesion, the greater the mining height is, the greater the plastic zone depth is, and the plastic zone depth is basically linearly positively correlated with the mining height

(2) When $m = 8$ m, $P_i = 0.1$ MPa, and $\varphi = 24°$, as shown in Figure 3(b), with the same cohesion, the greater the mining depth is, the greater the plastic zone depth is, and the relationship between the plastic zone depth and the mining depth is approximately hyperbolic, while at the same mining depth, the greater the coal cohesion, the smaller the plastic zone width

(3) When $H = 500$ m, $P_i = 0.1$ MPa, and $m = 8$ m, as shown in Figure 3(c), with the same cohesion, the greater the internal friction angle, the smaller the plastic zone depth, but the plastic zone depth decreases slightly with the increase in the friction angle; at the same internal friction angle, the plastic zone depth decreases with the increase in cohesion, and the reduction amplitude is obvious

(4) When $H = 500$ m, $m = 8$ m, and $\varphi = 24°$, as shown in Figure 3(d), with the same cohesive force, the greater the applied force is, the smaller the depth of plastic zone is. The depth of the plastic zone decreases with the increase in the applied force

The depth of the plastic zone in the coal wall determines the damage degree. The analysis shows that mining depth, mining height, and coal strength have significant influence on the development range of plastic zone. In order to control the instability of surrounding rock in stope, measures such as reducing mining height, grouting reinforcement, and increasing support resistance are adopted in practice.

4. Synchronous Instability Mechanism of the Direct Roof and Coal Wall

4.1. Failure Mode of the Coal Wall. Practice shows that the trace of coal wall spalling is closely related to coal hardness, gangue property, and support strength. If the coal mass is homogeneous, the joints and fissures are not developed, the hardness is small, and there is a large vertical stress acting on the coal wall, which is easy to form the arc-shaped crack to expand to the free surface of the coal wall; then, the synchronous instability as shown in Figure 4(a) is formed. When the strength of coal and direct roof is high, the coal wall is easy to form oblique linear failure trace under the action of roof high pressure, as shown in Figure 4(b). When the coal body is homogeneous and has no influence on the gangue, the joints and fractures are not developed, the integrity is good, the hardness is large, and the support of the coal wall is not timely. The vertical stress causes lateral horizontal displacement of the coal wall, which leads to the failure of the coal wall to break the groove shape, as shown in Figure 4(c). When there are gangues in the coal, the spalling extends or interrupts irregularly at the position of the gangue, thus forming the type as shown in Figure 4(d). Through years of field observation and theoretical research, there are two basic types of coal wall failure: shear and tension, of which (a) and (d) are more than 80%, and type (c) (16%) (a) and (b) belong to shear failure. Type (c) failure is due to a layer of relatively strong rock in the coal seam, and its failure principle is still shear failure. In general, tensile failure often occurs in hard coal seam, and type (d) failure is very rare.

The coal roof of group A in Zhangji mine of Huainan is directly covered with medium fine sandstone, as shown in Figure 5. The horizontal bedding is developed, and there are argillaceous bands in the layer, containing argillaceous inclusions and organic membrane, as shown in Figures 6 and 7. The average thickness of coal seam is 7.2 m, the strength of the coal body is low, and the hardness is 0.8~1. During the mining process, the roof caving and coal wall spalling are serious, and it is difficult to give full play to the supporting role of the bracket. After the coal wall spalling, the unsupported roof area increases. Under the action of the advanced bearing pressure, the roof is easy to leak and fall, which further weakens the support function of the roof. It is difficult to use shearer or air pick to directly crush

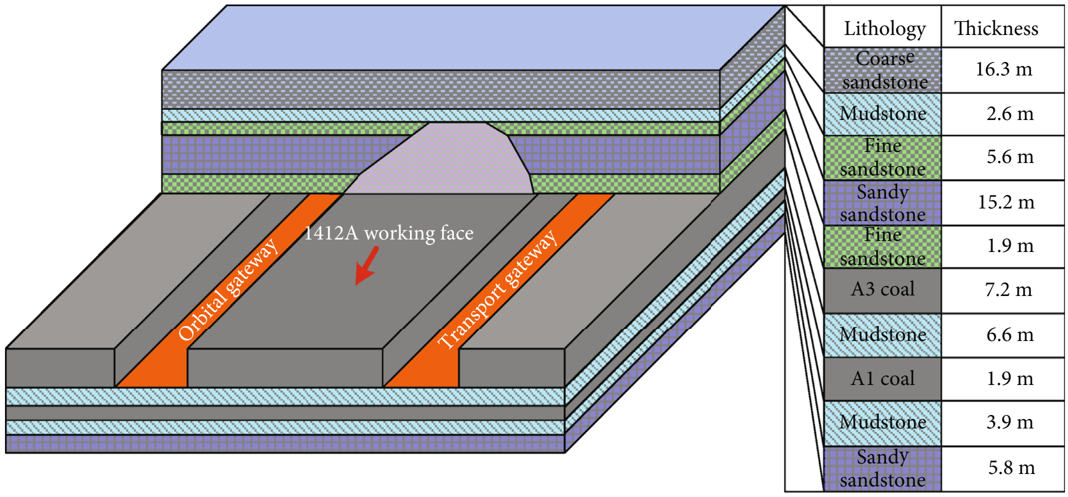

Figure 5: Working face layout and lithology histogram.

Figure 6: The sandstone intercalated with organic membrane.

the gangue due to its large size falling from the roof. It must be treated by drilling and blasting. The influence time is long, which further slows down the pushing progress of the working face, thus forming a vicious circle.

4.2. Synergistic Relationship Between Coal Wall Spalling and Roof Caving. Numerical and similar simulation tests show that the roof of the large mining height working face forms the overburden structure as shown in Figure 8. The stability of block B requires the support to provide supplementary load. The temporary balance of the structure just makes each working procedure of the mining operation successfully completed. Therefore, the stability of the overburden structure is determined by the large resistance of the support, especially for the working face with the mining height of 7~8 m. Due to the insufficient support force, the key blocks are prone to large swing or even sliding instability, which will lead to strong ore pressure appearance.

Due to the effect of advanced mining stress, the coal wall of soft and thick coal seam is prone to spalling, thus increasing the unsupported area. As shown in Figure 9, when the comprehensive roof control measures such as roof reinforcement and pressure relief are not adopted, the weak cohesive layer is separated by an organic membrane and argillaceous inclusion, and the open roof area exceeds the limit of stable span, and the composite layered roof falls in front of the support.

The support force is transmitted through the direct roof to control the change of overburden structure. When the roof caving height is large, the direct roof will be broken and the bearing capacity and stiffness will be reduced. As shown in Figure 10, the direct roof cannot transmit enough support force to the broken block B in this state, resulting in its reverse rotation, and the coal wall will not be able to provide the restraint force too, causing the support movable column to shrink down; it will aggravate the roof caving.

Figure 7: Argillaceous inclusions in sandstone.

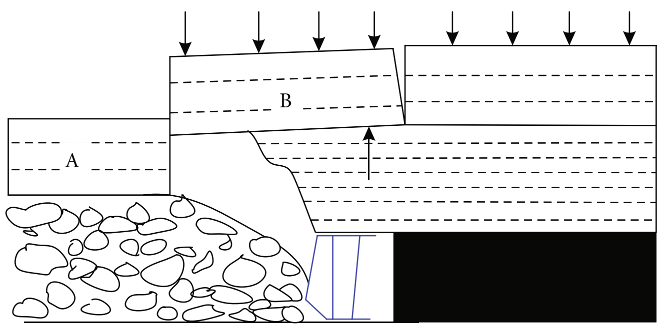

Figure 8: Normal mining.

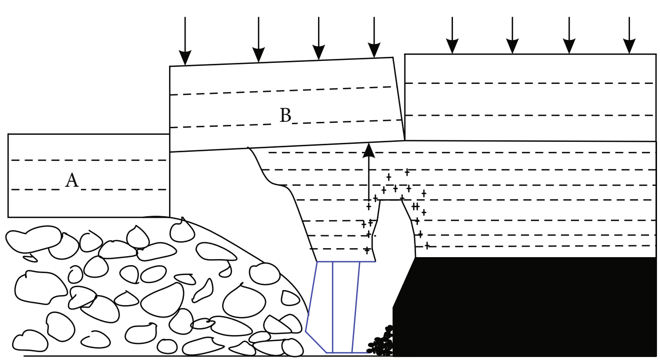

Figure 9: Roof caving caused by coal wall spalling.

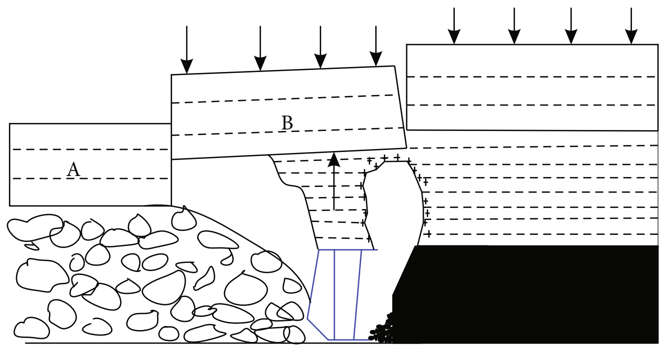

Figure 10: The change of roof structure aggravates the damage.

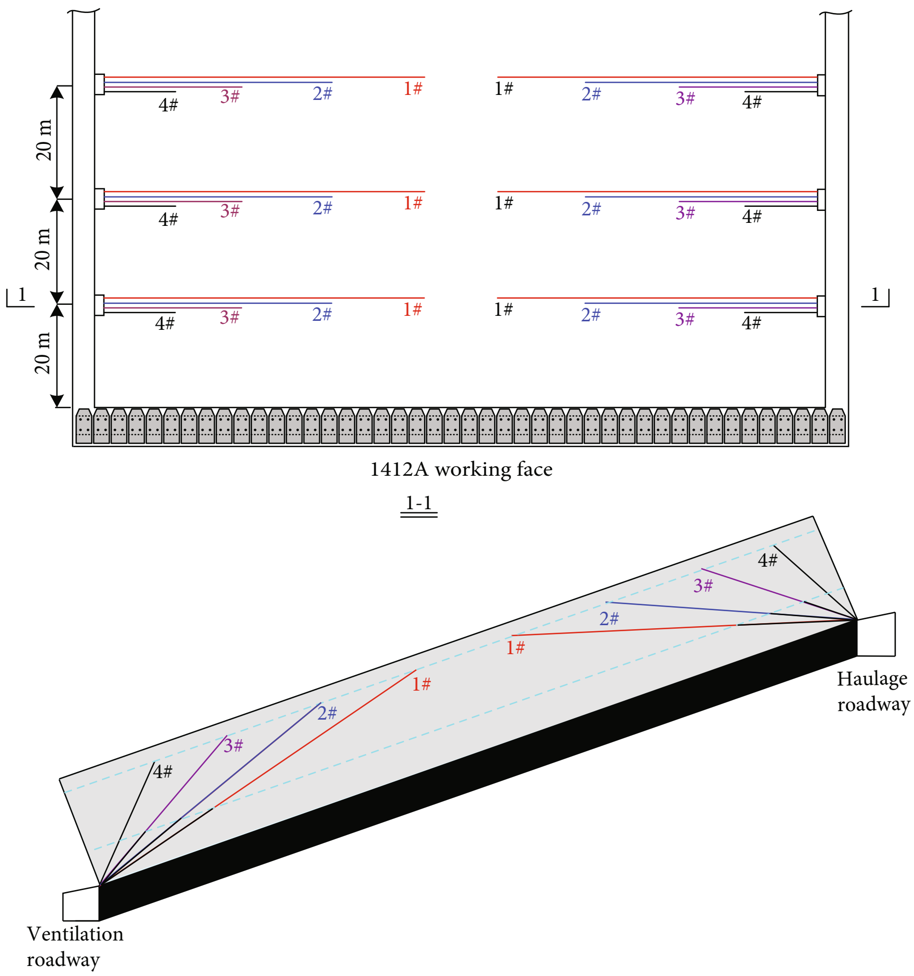

Figure 11: Layout of blasting hole cutting roof.

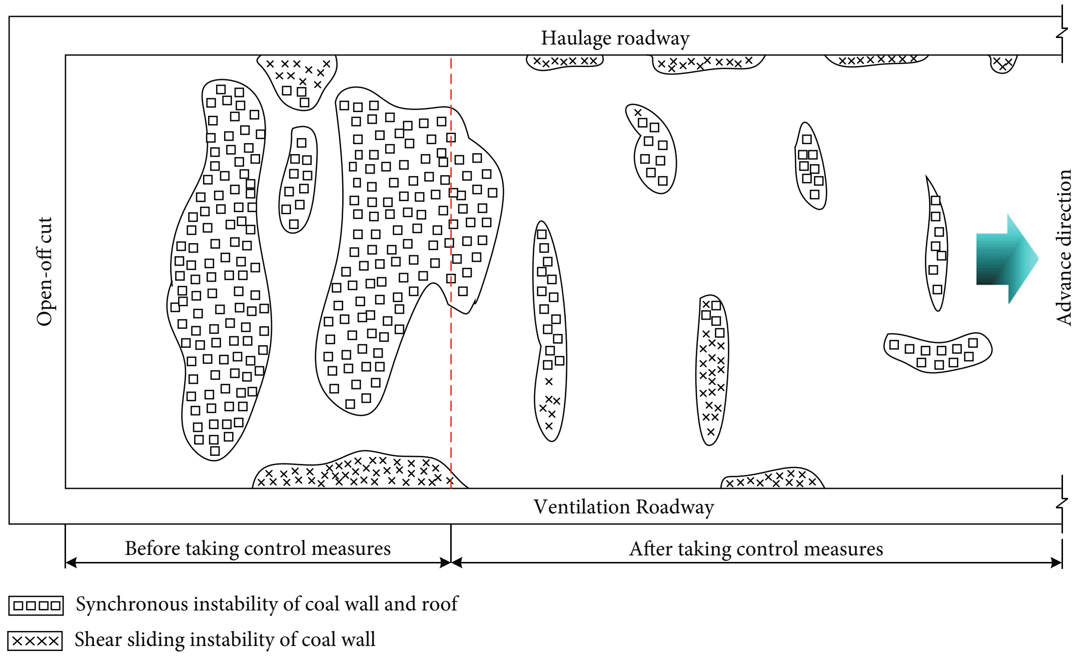

Figure 12: Comparison of working face control measures before and after.

5. Control of Coal Wall and Roof Synchronous Instability

In the process of mining in Group A of Zhangji mine, synchronous instability and strong ore pressure appear, which seriously affects the safety of working face. Through theoretical and practical research, the mechanism of surrounding rock instability in stope is expounded, and the comprehensive control measures of "cutting up and placing down" are adopted. Advanced mining stress is the key factor affecting the stability of the coal wall and roof, and the formation of mining stress is directly related to the overburden rock structure. By means of blasting presplitting, the key bearing rock blocks can be broken in advance, thus leading the advanced mining stress to act on the higher strata far away from the stope and weaken the impact on the direct roof and coal wall. According to the maximum bearing capacity of the support, the advance breaking distance is designed to make the hydraulic support effectively control the sinking of the direct roof and avoid the dynamic pressure influence on the coal wall and roof. According to the column chart, the 16.3 m coarse sandstone at the A3 roof is the key layer to control the ore pressure appearance, as shown in Figure 11.

In order to improve the strength and enhance its integrity, polymer materials are injected into the cracks or loose bodies by the pneumatic double liquid synchronous grouting pump, which consolidates and hardens the original broken, loose, and discontinuous rock mass into continuous and complete high-strength rock mass in a short time, so as to repair its defects in structure and improve the mechanical properties of surrounding rock mass. Through the treatment measures of "cutting up and pouring down", the frequency of roof caving and the depth of coal wall spalling are significantly improved, as shown in Figure 12.

6. Conclusion

(1) Based on the elastic-plastic theory, the mechanical model of coal wall stability analysis is established, and the analytical expressions of the stress and plastic zone about P_i, m, f, σ_c^*, C^*, φ, M_0, and S_z are obtained. Combined with mining conditions of A coal in Zhangji mine, it is shown that the mining depth, mining height, and coal cohesion have significant influence on the range of plastic failure zone, which directly determines the damage degree of coal wall spalling

(2) Coal strength of group A is low and easy to slide instability, thus increasing the unsupported space. Due to the influence of the mechanical membrane and argillaceous inclusions, the direct roof is prone to separation damage and then forms the synchronous instability. With the increase in the height of roof fall, the bearing capacity and stiffness of the broken direct roof will decrease, resulting in the reverse rotation of the broken key block, and the coal wall will not be able to provide the binding force at the end of the broken block, which will aggravate the spalling. The key block rotates and sinks, and roof caving is more serious

(3) The comprehensive control measures of "cutting up and injecting down" are adopted to improve the stability of the coal wall and direct roof. According to the maximum bearing capacity of the support, the

16.3 m thick coarse sandstone of A3 roof is pre-cracked with 10~15 m breaking distance from the two roadways, so that the advance mining stress is far away from the surrounding rock of the working face. In order to improve the strength and integrity of the roof, polymer materials are injected into the cracks or loose bodies of coal and rock mass to improve the mechanical properties

Data Availability

Others can access the data supporting the conclusions of the study from this research article. The nature of the data is the laboratory experimental data, the field observation data, and the theoretical calculation data. The laboratory experimental data used to support the findings of this study are included within the article; mainly, the mechanical parameters used to support the findings of this study are available from the corresponding author upon request.

Conflicts of Interest

The authors declare that they have no conflicts of interest.

Acknowledgments

The work presented in this paper is financially supported by the National Natural Science Foundation of China (Nos. 51674007, 52074008, and 52074007). The authors gratefully acknowledge the assistance of the Huainan Mining Group at the Anhui University of Science and Technology for providing access to the mine, data, and physical resources necessary to complete this work.

References

[1] Y. A. N. Shaohong, Y. I. N. Xiwen, G. J. Hu, and Q. M. Liu, "Roof structure of short cantilever-articulated rock beam and calculation of support resistance in full-mechanized face with large mining height [J]," *Journal of China Coal Society*, vol. 36, no. 11, pp. 1816–1820, 2011.

[2] F. Xinqiu, H. Jie, and L. Haichao, "A study of the coal wall fall mechanism in soft coal and its control at a fully-mechanized top-coal caving face," *Journal of China University of Mining Technology*, vol. 38, no. 5, pp. 640–644, 2009.

[3] W. Jiacheng, "Mechanism of the coal wall spalling and the controlling in the very soft coal seam," *Journal of China Coal Society*, vol. 32, no. 8, pp. 785–788, 2007.

[4] W. Jilin, Y. Yong, T. Shihao, and L. I. Bo, "Roof structure characteristics in fully mechanized coalface with large mining height and reasonable loading of support," *Journal of Mining and Safety Engineering*, vol. 31, no. 4, pp. 512–518, 2014.

[5] Y. Yong, T. Shihao, W. Ying, X. T. Ma, and Q. Wu, "Discussion on key problems and countermeasures of fully mechanized mining technology with high mining height," *Coal Science and Technology*, vol. 38, no. 1, pp. 4–8, 2010.

[6] H. Junxiao, L. Huamin, X. Zuoqiang, and W. Wang, "Analysis on setting load and stope control at overlength long face with large mining height in Sihe coal mine," *Coal Technology*, vol. 29, no. 12, pp. 74-75, 2010.

[7] Y. Shaohong, Y. Xiwen, G. J. Hu, and Q. M. Liu, "Roof structure of short cantilever-articulated rock beam and calculation of support resistance in full-mechanized face with large mining height," *Journal of China Coal Society*, vol. 36, no. 11, pp. 1816–1820, 2011.

[8] H. Qingxiang, *Study on roof structure and strata control of long wall mining in shallow seam*, China University of Mining and Technology Press, Xuzhou China, 2000.

[9] W. Guofa, L. Junfeng, and R. Huaiwei, "Design and optimization of high seam-caving coal hydraulic support based on model of support and wall rock coupling," *Journal of China Coal Society*, vol. 36, no. 1, pp. 145–151, 2011.

[10] W. Xuejun, Q. Xuesen, and M. Liqiang, "Research on large mining height technique for thick coal seams," *Journal of Mining and Safety Engineering*, vol. 26, no. 2, pp. 212–216, 2009.

[11] H. Haijin, W. Jian, Z. Yong, and Z. B. Yuan, "The balance structure of main roof and its action to immediate roof in large cutting height workface," *Journal of China Coal Society*, vol. 29, no. 2, pp. 137–141, 2004.

[12] Y. Shaohong and Y. Xiwen, "Discussing about the main theoretical problems of long wall with top coal caving," *Journal of China Coal Society*, vol. 33, no. 5, pp. 481–484, 2008.

[13] W. Jiacheng and W. Zhaohui, "Stability of main roof structure during the first weighting in shallow high-intensity mining face with thin bedrock," *Journal of Mining and Safety Engineering*, vol. 32, no. 2, pp. 175–181, 2015.

[14] W. Jiacheng, Z. Jian, and J. Liuting, "Study on mechanics model of the first cave in main roof for the large cutting height fully mechanized mining under the two hard conditions," *Chinese Journal of Rock Mechanics and Engineering*, vol. 24, pp. 5037–5042, 2005.

[15] H. Guowei and J. Zhongming, "Practice of pressure law and study on the strata behavior regularity of large mining height fully-mechanized face," *Journal of Taiyuan University of Technology*, vol. 37, no. 2, pp. 127–130, 2006.

[16] G. Peiling and J. Zhongming, "Research on influencing factors of tilt for fully-mechanized mining support with large mining height," *Journal of Taiyuan University of Technology*, vol. 32, no. 6, pp. 666–669, 2001.

[17] Y. Bo, M. Xiangrui, Z. Guangming, and G. Zhaoning, "Research on swallow-tailed catastrophe model of coal wall spalling in fully mechanized caving face with great mining height for soft coal seam," *Coal*, vol. 21, no. 1, pp. 1–4, 2012.

[18] Y. Bo, "Study on mechanism and control technology of coal wall spalling in fully mechanized caving face with great mining height of three-soft coal seam," Anhui University of Science and Technology, Anhui China, 2012.